

Single Neutral Pion Production by Pions at 1100 Mev*

V. P. KENNEY,† W. D. SHEPHARD, AND C. D. GALL‡
University of Kentucky, Lexington, Kentucky

(Received November 17, 1961; revised manuscript received December 21, 1961)

Well-identified events of the type $\pi^- + p \rightarrow p + \pi^- + \pi^0$ were obtained by requiring, in addition to satisfaction of kinematic criteria, that the production of the neutral pion be verified by observation of either a γ -ray conversion electron pair or a Dalitz-decay pair associated with the interaction. In a scan of 100 000 Bevatron photographs 70 acceptable events were found. The kinematic behavior of the selected events did not agree with the predictions of the isobar model, but was consistent with the assumption that the events were initiated by a strong pion-pion interaction, with subsequent rescattering of pions by the nucleon. There is some indication that two $T=1$ dipion states with total energies of 565 and 750 Mev are involved in the interactions.

I. INTRODUCTION

ATTEMPTS to understand the mechanism by which pions are produced in pion-nucleon scattering may be characterized phenomenologically in two ways. The primary pion may be regarded as interacting with the nucleon as a whole, or the detailed structure of the nucleon may be considered. In the latter case, processes involving the nucleon "core" may be distinguished from those which involve the "pion cloud" of the physical nucleon.

The isobar model of Lindenbaum and Sternheimer¹ describes phenomenologically a mechanism in which an incident pion excites the physical nucleon to a metastable "isobaric state" of rather well-defined energy, which decays by pion emission to the ground state. This model has recently been extended² to describe interactions which proceed either through the isospin- $\frac{3}{2}$ state, with excitation energy (Q value) 146 Mev, or through one of two isospin- $\frac{1}{2}$ states, with excitation energies 434 Mev and 593 Mev, respectively. The "statistical model"³ in which the relative probabilities of final states are calculated from the available phase space has been applied with considerable success to multi-Bev reactions by Hagedorn,⁴ who includes the effect of final-state $\pi-N$ interactions. Pion production may also be considered in terms of interaction between the incident pion and an individual pion in the "pion cloud" of the nucleon with or without rescattering of the final-state pions by the nucleon.⁵⁻¹⁰

One might hope that in a given energy range only one of these phenomenological mechanisms would be important and that the importance of a given mechanism might be determined by the extent to which the wave function describing the incident pion overlaps that of the physical nucleon. Unfortunately such a well-defined separation does not seem possible. Evidence for the importance of the pion-pion interaction at the pion production threshold^{11,12} and at energies well above the threshold for strange particle production,¹³ a characteristic "core" interaction, would indicate that the task of distinguishing the pion production mechanism may be very difficult. Recent experimental studies¹⁴⁻¹⁸ of the reactions

$$\pi^- + p \rightarrow p + \pi^- + \pi^0: [“(p\pi^- \pi^0)”] \quad (1)$$

and

$$\pi^+ + p \rightarrow n + \pi^+ + \pi^-: [“(n\pi^+ \pi^-)”], \quad (2)$$

near 1 Bev, have indicated that while reaction (2) appears reasonably consistent with the kinematic predictions of the isobar model, the character of reaction (1) is open to some doubt. The results of Derado and Schmitz¹⁴ indicate that in reaction (1) the π^- mesons have appreciably lower momentum than the π^0 , and that the reaction kinematics can be interpreted⁶⁻⁸ as primarily due to a resonant pion-pion interaction. Results from other groups,¹⁵⁻¹⁸ however, would seem to show that the momentum distribution of the π^- mesons peaks at higher values than that of the π^0 , as would be expected if the reaction proceeds predominantly through excitation of the $T=J=\frac{3}{2}$ isobar.

The significance of a possible difference in the mechanisms of reactions (1) and (2) is evident from the

¹¹ W. A. Perkins, J. C. Caris, R. W. Kenney, and V. Perez-Mendez, Phys. Rev. **118**, 1364 (1960).

¹² L. S. Rodberg, Phys. Rev. Letters **3**, 58 (1959).

¹³ A. R. Erwin, R. March, W. D. Walker, and E. West, Phys. Rev. Letters **6**, 628 (1961).

¹⁴ I. Derado and N. Schmitz, Phys. Rev. **118**, 309 (1960).

¹⁵ V. Alles-Borelli, S. Bergia, E. Perez Ferreira, and P. Waloschek, Nuovo cimento **14**, 211 (1959).

¹⁶ E. Pickup, F. Ayer, and E. O. Salant, Phys. Rev. Letters **5**, 161 (1960).

¹⁷ E. Pickup, D. K. Robinson, and E. O. Salant, *Proceedings of the 1960 Annual International Conference on High-Energy Physics at Rochester* (Interscience Publishers, Inc., New York, 1960), p. 72.

¹⁸ J. G. Rushbrooke and D. Radojicic, Phys. Rev. Letters **5**, 567 (1960).

* Research supported by the National Science Foundation, and carried out in collaboration with the Alvarez bubble chamber group of the Lawrence Radiation Laboratory.

† On leave 1961-62 at the Max-Planck-Institute for Physics, Munich, Germany.

‡ Now at the Mohawk Valley Technical Institute, Utica, New York.

¹ S. J. Lindenbaum and R. M. Sternheimer, Phys. Rev. **109**, 1723 (1958).

² S. J. Lindenbaum and R. M. Sternheimer, Phys. Rev. Letters **5**, 24 (1960); R. M. Sternheimer and S. J. Lindenbaum, Phys. Rev. **123**, 333 (1961).

³ E. Fermi, Progr. Theor. Phys. (Kyoto) **5**, 570 (1950).

⁴ R. Hagedorn, Nuovo cimento **15**, 434 (1960); Fortschr. Physik **9**, 1 (1961).

⁵ W. R. Frazer and J. Fulco, Phys. Rev. **117**, 1609 (1960).

⁶ F. Bonsignori and F. Selleri, Nuovo cimento **15**, 465 (1960).

⁷ I. Derado, Nuovo cimento **15**, 853 (1960).

⁸ F. Selleri, Nuovo cimento **16**, 775 (1960).

⁹ R. F. Peierls, Phys. Rev. **118**, 325 (1960).

¹⁰ P. Carruthers and H. Bethe, Phys. Rev. Letters **4**, 536 (1960).

discussions of the one-pion exchange process for pion production by Peierls¹⁹ and by Carruthers.²⁰ The question of whether the experimental evidence does or does not support such a difference is, then, a most interesting one, and provides the motivation for the investigation of single neutral pion production which is described here.

II. IDENTIFICATION OF SINGLE NEUTRAL PION PRODUCTION EVENTS

One of the most difficult experimental problems is the establishment of procedures by means of which two-prong events which do not satisfy elastic-scattering kinematic tests may be identified as belonging to one of the inelastic-scattering reactions (1) or (2). McCormick and Baggett²¹ have pointed out that the usual χ^2 separation criteria based on interaction kinematics become less useful as the momenta of the positive and neutral particles approach the same value. No kinematic separation at all is possible in the limiting case where the positive and neutral momenta are equal, even with infinite measurement precision. Since measurements are made with finite precision, the ambiguity may extend to an appreciable fraction of single-pion production events at these energies. This question has been explored in detail by Derado, Lutjens, and Schmitz,²² who found that, in the pion production experiment referred to previously,¹⁴ the kinematic separation of reactions (1) and (2) was not possible in some 25% of the events.²³

One might still hope to distinguish these reactions by means of the characteristics of the positive particle track in each case. The velocity dependence of the bubble density for tracks in hydrogen is known,²⁴ and it is in principle possible to distinguish between protons and positive pions having the same momenta by the appearance of the tracks. In practice, such a separation depends very much on the operating conditions of the bubble chamber.

Track density depends not only on the particle velocity, but on the temperature and pressure at which the bubble chamber is run, and a chamber can be operated so that even "minimum density" tracks are essentially continuous. In most pion experiments to date, pion production has been studied in bubble chamber photographs primarily intended for the study of strange particle production. Consequently, in these photographs it was desirable to keep the tracks of the fast beam particles

quite dense to reduce the end-point uncertainty in the neutral "V" production.

This presents a serious problem for the separation of the inelastic-scattering reactions. In the region of maximum kinematic ambiguity, ~ 600 Mev/ c , pion and proton track densities differ at most by a factor of 2. In the bubble chamber photographs available for this experiment the beam tracks themselves were comparatively dense. Dip angle foreshortening of the bubble gaps and temperature variations in the chamber further reduce the reliability of reaction identifications based on the relative track densities. Derado and Schmitz,²⁵ for example, found that in the region of kinematic ambiguity all tracks had bubble densities in the range 20 cm^{-1} to 25 cm^{-1} , and that no momentum dependence whatsoever could be established. They developed, consequently, a δ -ray measurement technique for the identification of pions and protons, which was comparatively independent of the operating conditions of the bubble chamber. The selection criteria adopted by other groups who have been faced with this problem are not well known, and may vary widely.

In the present experiment the problem of kinematic ambiguity was avoided by selecting a restricted sample of ($p\pi^-\pi^0$) events, in which the identification was made by requiring the observation of a conversion electron pair correlated with the interaction in addition to the satisfaction of conventional kinematic and track density criteria. Since the radiation length of liquid hydrogen is 9.9 m and the radius of the bubble chamber only 5 in., this selection procedure severely limits the statistics possible in such an experiment. Inasmuch as the characteristics of reaction (1) have already been reported with moderately good statistics by several authors,¹⁴⁻¹⁸ and since the present purpose is to investigate only the most obvious differences among these reports, the statistical limitations do not present serious difficulties.

The possibility of bias in the selection criterion based on observation of a conversion electron pair is a more serious problem. A group of "four prong" events involving Dalitz-decay of the π^0 , in which the pair is produced directly at the interaction vertex, has been included in the study. This group of events should be free of any scanning bias and can be compared with the group of events involving conversion pairs. The "four-prong" events, which also helped to improve the statistics of the experiment, were selected in a companion study of multiple pion production by pions.²⁶

III. SCANNING AND MEASUREMENT PROCEDURE

Approximately 100 000 stereo pairs of photographs of the Alvarez 10-in. hydrogen bubble chamber, set up in a 1.24-Bev/ c negative pion beam at the Bevatron,

¹⁹ R. F. Peierls, Phys. Rev. Letters **5**, 166 (1960).

²⁰ P. Carruthers, Phys. Rev. Letters **6**, 567 (1961).

²¹ L. Baggett, University of California Lawrence Radiation Laboratory Report UCRL-8302 (unpublished).

²² I. Derado, G. Lutjens, and N. Schmitz, Ann. Physik **4**, 103 (1959).

²³ One can, nonetheless, make a kinematic identification in that fraction of the events in which the positive pion comes off with scattering angle greater than the maximum angle permitted for the proton, as discussed by R. Sternheimer, Phys. Rev. **93**, 642 (1954).

²⁴ V. P. Kenney, Phys. Rev. **119**, 432 (1960).

²⁵ I. Derado and N. Schmitz, Nuovo cimento **11**, 887 (1959).

²⁶ V. P. Kenney, J. G. Dardis, and G. Brunhart Phys. Rev. **124**, 1568 (1961).

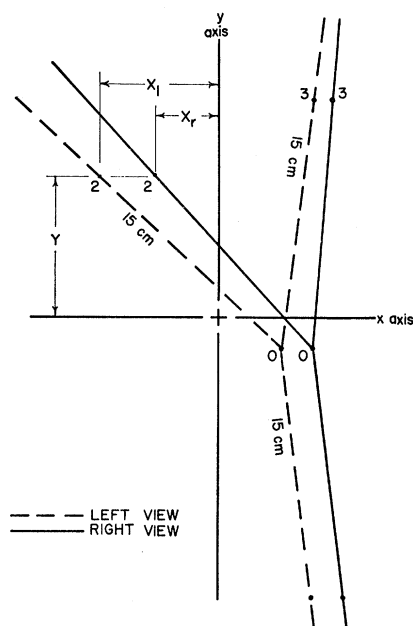


FIG. 1. A typical configuration of tracks in two stereo views when the central fiducial mark in each view is superimposed.

were scanned for 2-prong events with correlated conversion pairs. Each frame was independently scanned in both views by two observers, and each possible event was measured independently by four observers whose results were monitored for consistency.

A two-lens stereo projector, with which the views could be presented singly or superimposed on a ground glass screen, was used to facilitate scanning and measuring. The projector optics were similar to the original camera optics. The right-hand lens was continuously movable in a plane perpendicular to the stereo axis so that corresponding points in the two views could be brought into coincidence on the screen. The observer could visually reconstruct spatial relationships between events in the chamber by placing appropriately oriented Polaroid disks in front of the projector lenses and wearing spectacles with similarly oriented Polaroid lenses. By varying the position of the movable lens, the scanner could examine different planes in the chamber such as the planes of the front and back windows or the plane containing the interaction vertex and could readily determine whether an electron pair appeared sufficiently correlated with an interaction to warrant detailed measurements. The geometrical orientations of the events selected were checked subsequently in the detailed analysis.

The selected events were measured according to the following procedure:

- (a) The chord length of each track was measured.
- (b) The radius of curvature of each track was independently measured in two ways; (1) using templates of transparent plastic inscribed with standard railroad

curves and tangent marks, and (2) using a magnifying glass mounted with a reticle with 0.1-mm scale divisions to measure the sagitta of the curve.

(c) The views were superimposed so that the center fiducial mark of the front glass plane coincided in the two views.

(d) A tangent line was drawn to each track using the template marks.

(e) The coordinates of the interaction point and reference points 15-cm distant along the track tangents were measured in each view, as shown in Fig. 1.

From the original lens separation, the distance of the lenses from the front glass of the chamber, and the refractive index of hydrogen, the coordinates of each reference point with respect to the center fiducial mark may then be calculated. When a coordinate rotation to the reference frame of the incoming track is effected, the space angles of the initial direction of each outgoing track may then be calculated in first-order optics. The momenta were calculated from the measured radii of curvature and the magnetic field at the depth of the center of the track. An IBM-650 computer was used to carry out these calculations.

The accuracy of the momentum measurement depends on the length of the track. Four independent measurements of the radius of curvature of a track 10-cm long in the chamber typically agreed within $\sim 10\%$. Coordinate measurements agreed within ~ 0.05 cm (chamber dimensions). Since turbulence in the small 10-in. chamber limits measurement accuracy, the suppression of systematic error was emphasized. The measurement accuracy achieved was considered adequate for the purpose of the experiment.

IV. ANALYSIS

A total of 62 possible single neutral pion production events were initially selected on the basis of the associated electron pair criterion in the scan of 10^5 bubble chamber photographs. To these were added 33 events which would not be identified as

$$\pi^- + p \rightarrow p + \pi^+ + \pi^- + \pi^- : [“(p\pi^+\pi^-\pi^-)”],$$

in the companion study of multiple pion production, and which had tracks which appeared consistent with electron pairs from Dalitz-decay. The two groups are referred to as “type A” events and “type B” events, respectively, in the discussion which follows.

These 95 events were tested for consistence with single pion production kinematics, and events were eliminated in which the positive particle scattering angle exceeded the maximum proton recoil angle for this energy, or in which the calculated neutral particle mass was not consistent with the known π^0 mass within the limits determined from measurement uncertainties.

Tentative identifications were assigned to the 25 events which were not ($p\pi^-\pi^0$) cases by calculating kinematic limits on the value of the missing neutral

TABLE I. Event classification in the present experiment.

Event classification	Type A	Type B	Total events
$p\pi^-\pi^0$	45	25	70
$n\pi^+\pi^-$	2	0	2
$p\pi^-\pi^0\pi^0$	5	0	5
$n\pi^+\pi^-\pi^0$	7	7	14
Other	3	1	4
Total	62	33	95

mass, by identifying π^+ tracks for which the scattering angle exceeded the maximum proton recoil angle, and by considering relative track densities and momenta. The resulting classifications are summarized in Table I. The "other" category in this table includes two elastic π^- , p scatterings, one ($n\pi^0\pi^0$) event with an electron pair at the vertex and a related conversion pair, and one previously unidentified four-prong event of the type ($p\pi^-\pi^-\pi^+$).

Of the 25 events which were not ($p\pi^-\pi^0$), the identification was relatively certain in 15 cases and somewhat ambiguous in 10. In the two elastic events and the two single positive pion production events, the selected "correlated conversion electron pairs" were found to be low-energy background pairs in two cases, and accidental directional correlation of presumably good π^0 -decay conversion pairs in the two others.

In any comparison of single pion production and multiple pion production from the data of Table I, it should be emphasized that the 62 "type A" events, and the 33 "type B" events were selected from different samples of data at different times by different people, and that no direct comparison between them should be made.

Although the number of events selected in this experiment is small, the results are of interest since comparisons may be made with other pion production experiments in which differing conclusions have been reached. The results also provide information on the characteristics of events obtained by requiring the presence of a correlated electron pair and evidence about the advantage and/or limitations of this selection technique.

V. EXPERIMENTAL RESULTS

The quantities of interest calculated in this study include the scattering angle and momentum of each final-state particle, including the neutral particle, in the pion-proton center-of-mass system (c.m.s.); the c.m.s. space angles between two particles for various pairs of emitted particles; and values of $Q = (E^{*2} - p^{*2})^{1/2} - (m_1 + m_2)$, the sum of the kinetic energies of two particles in the c.m.s. of the two particles, for various possible two-body intermediate states.

The angle distribution of the protons from the neutral pion production events is shown in Fig. 2, and the angle

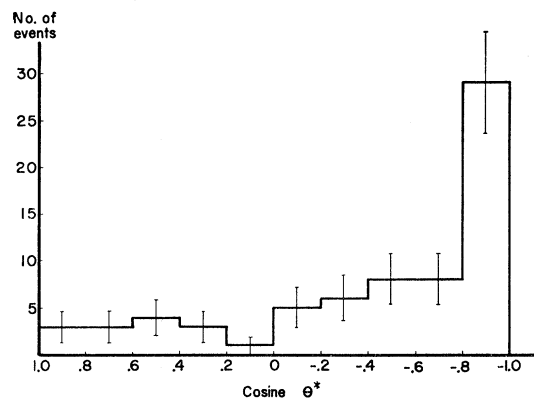


FIG. 2. Scattering-angle distribution for the proton from the ($p\pi^-\pi^0$) production reaction in the c.m.s.

distributions for the two pions are shown in Fig. 3. Some 80% of the nucleons emerge from the reaction in the backward c.m. hemisphere. The π^0 angle distribution is peaked sharply forward, while the π^- distribution is more or less isotropic.

The distributions of angles between particles in pion-proton and pion-pion pairs are shown in Fig. 4 and Fig. 5, respectively. The angle between the π^0 and proton is generally large; except for a decided excess in the interval $-0.8 < \cos\psi^* < -1.0$, the distribution in angles between the π^- and proton is nearly isotropic. The distribution of the angles between the pions is not sharply peaked, but favors angles greater than 90° .

The proton c.m. momentum distribution, Fig. 6, shows a broad peak between 300–550 Mev/c. The π^- and π^0 momentum distributions are both shown in Fig. 7, along with the predictions of the statistical model. The neutral pion momentum distribution peaks at ~ 500 Mev/c, well above the peak of the π^- momentum distribution which is at ~ 250 Mev/c. The distributions for the 25 "type B" events, selected on the basis of a Dalitz-decay pair at the event vertex, are plotted with

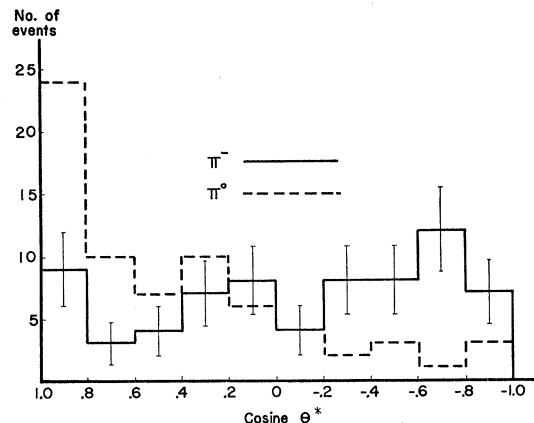


FIG. 3. Scattering-angle distributions for the pions from the ($p\pi^-\pi^0$) production reaction in the c.m.s.

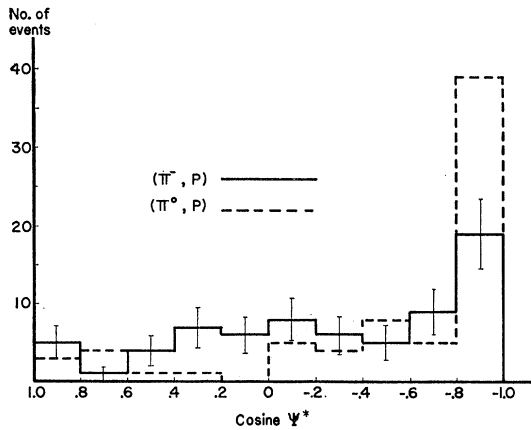


FIG. 4. Distributions of angles between the pions and the nucleon from the $(p\pi^-\pi^0)$ production reaction in the c.m.s.

dashed lines, and these seem to show the same features as the total distributions.

The pion-proton Q -value distributions in Fig. 8, show that the (π^-, p) Q values have a peak below 150 Mev, while the (π^0, p) Q values rise to a peak near 450 Mev.

VI. NUCLEON ISOBAR ANALYSIS

Single-pion production experiments have been widely interpreted¹⁴⁻¹⁷ in terms of an isobar model, as indicated schematically in Fig. 9 in the c.m.s. of the original pion

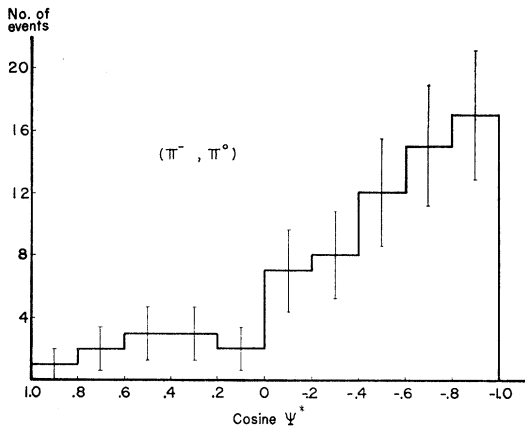


FIG. 5. Distributions of angles between pions from the $(p\pi^-\pi^0)$ production reaction in the c.m.s.

and proton. The production of a three-body final state is treated in terms of two-body processes; the initial pion-proton interaction yields a "recoil" pion and an isobar which subsequently decays into a final-state nucleon and a "decay" pion.

The kinematic behavior expected of the reaction products depends sensitively on the mass of the isobar. If, for example, the isobar is identified with the $T=J=\frac{3}{2}$ resonant state observed in low-energy pion-nucleon scattering, it may be assigned an effective mass

$M_{\frac{3}{2}}^* = 1225$ Mev, corresponding to a Q value of 145 Mev for decay into a pion-proton pair. The following characteristics would be consistent with production of the $T=J=\frac{3}{2}$ isobar at the energy of this experiment: (1) The comparatively small excitation energy of the isobar requires relatively little momentum transfer

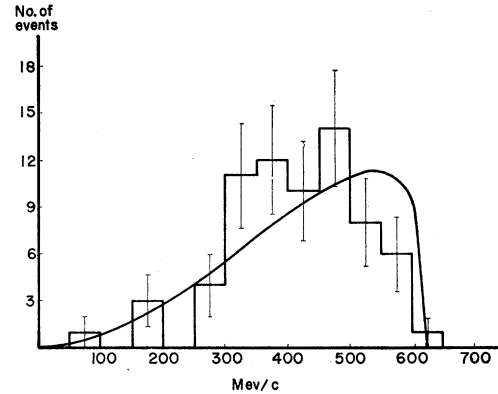


FIG. 6. Proton momentum distribution in the c.m.s. The smooth curve is the phase-space distribution plotted for comparison.

from the incoming pion, so the recoil pion might be predominantly fast and forward-scattered in the pion-proton c.m.s.; (2) the final nucleon from the isobar decay would carry off most of the isobar momentum, and would tend to go backward in the pion-proton c.m.s. at large angles with respect to the recoil pion;

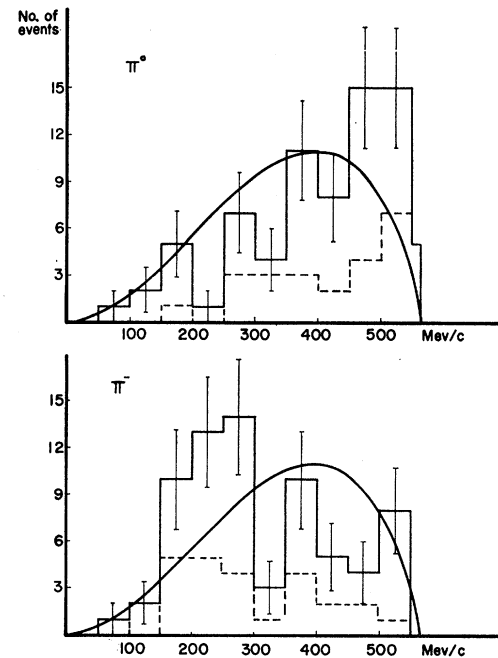


FIG. 7. Momentum distributions for the neutral (top) and negative (bottom) pions in the c.m.s. Distributions for the type-B events only, in which the neutral pion decayed with Dalitz internal conversion, are shown by the dotted histograms. The curve obtained from phase-space dependence alone is plotted for comparison.

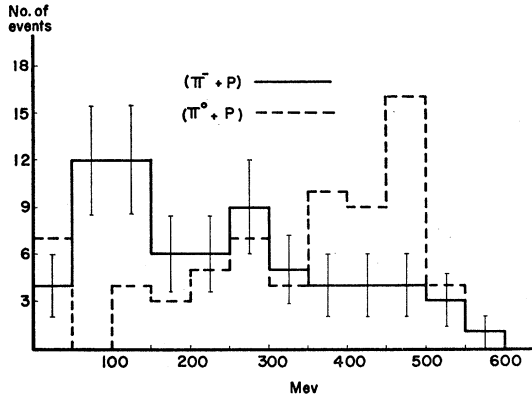


FIG. 8. Pion-proton Q values for the $(p\pi^-\pi^0)$ production reaction.

(3) the decay pion from the isobar would be left with a much lower momentum than the recoil pion, and would tend to emerge at large angles with respect to the recoil pion. The distribution of angles between decay pion and nucleon would be more nearly symmetrical about 90° with some predominance of angles less than 90° .

If it is assumed that the peak in the π^-, p total cross section observed at 600 Mev²⁷⁻²⁸ is associated with a more highly excited $T=\frac{1}{2}$ isobar with mass $M_{\frac{1}{2}}^*=1510$ Mev, corresponding to a Q value of 435 Mev, and that this isobar is excited in pion production interactions near 1 Bev, a rather different type of kinematic behavior would be expected. Since production of this more highly excited isobar would require a considerable momentum transfer from the incoming pion: (1) The recoil pion

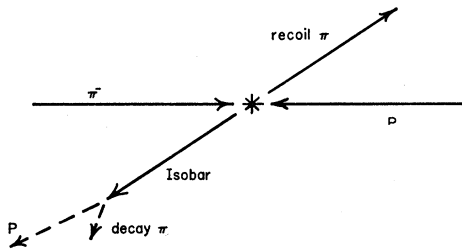


FIG. 9. Center-of-mass schematic drawing of isobar production and decay.

would now be relatively low in momentum and would not necessarily be strongly forward-scattered; (2) the more massive isobar would tend to be slow and to decay near the pion-proton interaction point, so the final nucleon would come off more or less isotropically with respect to the slow recoil pion, but probably would tend to go in the backward hemisphere; (3) the decay pion from the more highly excited isobar would be

²⁷ T. J. Devlin, B. C. Barish, W. N. Hess, V. Perez-Mendez, and J. Solomon, Phys. Rev. Letters 4, 242 (1960).

²⁸ J. C. Brisson, J. Detoef, P. Falk-Vairant, and L. Van Rossum, Phys. Rev. Letters 3, 561 (1959); P. Falk-Vairant and G. Valadas, Proceedings of the 1960 Annual International Conference on High-Energy Physics at Rochester (Interscience Publishers, Inc., New York, 1960), p. 38; Revs. Modern Phys. 33, 362 (1961).

considerably faster than, and more or less isotropic in direction with respect to the recoil pion; its direction would, however, tend to be opposite to that of the final nucleon, so that, if the nucleon is back-scattered, the recoil pion would be scattered forward.

The kinematics of isobar formation and decay have been studied in detail by Lindenbaum and Sternheimer.¹⁻² Figure 10 shows the momentum spectra for the decay and recoil pions from both $T=\frac{3}{2}$ and $T=\frac{1}{2}$ isobar formation, as predicted by the Lindenbaum-Sternheimer model for an incoming pion energy of 1100 Mev. It is clear that the spectrum for the "slow" decay pion from $T=\frac{3}{2}$ isobar formation ($J_{\pi,1}$) peaks at very nearly the same momentum value, ~ 250 Mev/ c , as the spectrum for the "slow" recoil pion from $T=\frac{1}{2}$ isobar formation ($J_{\pi,3}$). Similarly the spectrum of the

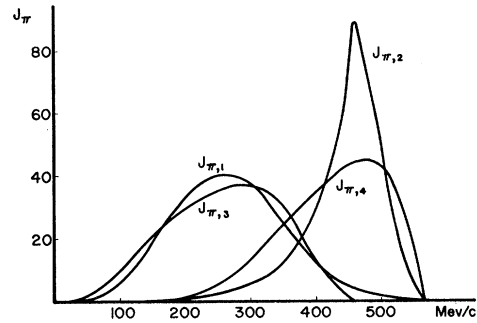


FIG. 10. Center-of-mass momentum spectra of pions from the 1100-Mev pion production reaction, obtained on the isobar model by neglecting the low-energy $T=\frac{1}{2}$ cross section.

"fast" recoil pion from $T=\frac{3}{2}$ isobar formation ($J_{\pi,2}$) and the spectrum of the "fast" decay pion from $T=\frac{1}{2}$ isobar formation ($J_{\pi,4}$) peak at the same momentum value, ~ 450 Mev/ c . This is very largely due to the values which are assumed for $M_{\frac{3}{2}}^*$ and $M_{\frac{1}{2}}^*$. The same discussion applies to Fig. 11, which shows momentum spectra for the same pions as in Fig. 10, but includes effects of the $T=\frac{1}{2}$ cross section at low energies.²

It follows that although the principal kinematic

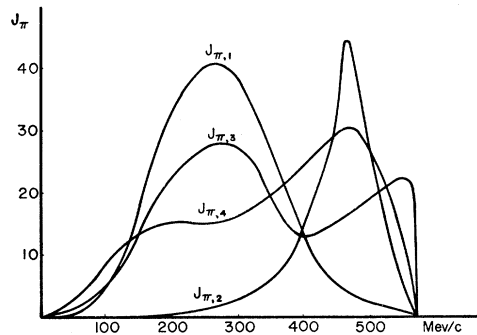


FIG. 11. Center-of-mass momentum spectra of pions from the 1100-Mev pion production reaction, obtained for the isobar model by including the contribution of the low-energy $T=\frac{1}{2}$ cross section.

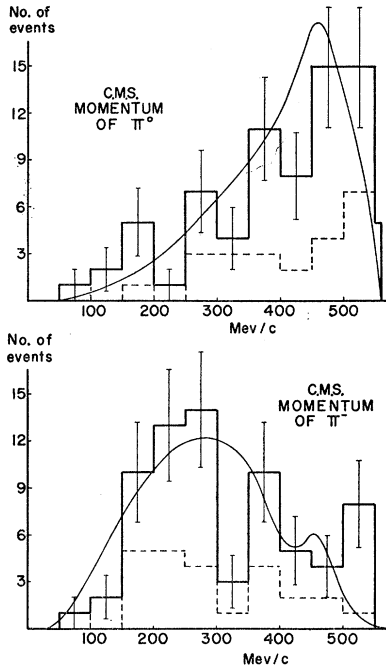


FIG. 12. Momentum distributions for the neutral and negative pions from the $(p\pi^-\pi^0)$ production reaction in the c.m.s. The dashed histogram includes only the type-B Dalitz decay events. The smooth curve is obtained from a preliminary calculation for the isobar model by setting $\sigma_{12}/(\sigma_{11}+\sigma_{12})=0.7$.

features observed in the present experiment are qualitatively consistent with an isobar model, no conclusions may be drawn from this agreement about the mixture of isotopic spin $\frac{3}{2}$ and $\frac{1}{2}$ states which must be assumed. The distribution of momenta, scattering angles, and correlation angles between pairs of particles observed here could be explained equally well from the point of view of isobar kinematics (neglecting, for the moment, the charge preferences determined by the isotopic spins of the isobars), by assuming that the π^0 was predominantly the fast recoil and the π^- the slow decay pion from $T=\frac{3}{2}$ isobar formation, or by assuming that the π^0 was predominantly the fast decay and the π^- the slow recoil pion from the $T=\frac{1}{2}$ isobar. The same ambiguity exists in the interpretation of Q -value distributions: The fact that the (π^-,p) distribution shows a peak below 150 Mev could perhaps be attributed to formation of the $T=J=\frac{3}{2}$ state; the fact that the distribution for (π^0,p) pairs shows at least as marked a peak in the vicinity of 450 Mev cannot, however, be simultaneously interpreted as an effect of the lower $T=\frac{1}{2}$ state. One can conclude only that each interaction tends to produce a fast and a slow pion with momentum distributions which peak as shown in Figs. 9-10.²⁹ One

²⁹ A somewhat different interpretation of Q -value information seems to be given by E. Pickup, F. Ayer, and E. O. Salant, *Phys. Rev. Letters* **5**, 161 (1960). These appear to be to some extent modified by the same authors in *Proceedings of the 1960 Annual International Conference on High-Energy Physics at Rochester* (Interscience Publishers, Inc., New York, 1960), p. 69.

finds, in fact, that the events whose computed (π^-,p) Q values fall in the low-energy peak are the same events whose computed (π^0,p) Q values fall in the high-energy peak.

Detailed analysis of the kinematic data in terms of the isobar model must, then, take into account the fact that the isotopic spins of the two isobars energetically possible at this energy should effectively determine the preferences for the high- and low-momentum pions of different charges. It is of interest that the results of the present experiment indicate that the π^0 meson is predominantly the faster of the two.

The manner in which detailed calculations may be carried out for the extended isobar model, which considers formation of both $T=\frac{3}{2}$ and $T=\frac{1}{2}$ isobars in pion production by pions at these energies, has been discussed by Sternheimer and Lindenbaum.² The calculations performed for this experiment will be summarized. As a first approximation, the expected momentum distributions for the π^0 and π^- from $(p\pi^-\pi^0)$ production were calculated from: (1) the known total cross sections for²⁸ π^-,p and³⁰ π^+,p inelastic scattering; (2) the ratio of the charge states $(p\pi^-\pi^0): (n\pi^+\pi^-)$ as measured at 1.0 Bev, assumed to be the same at 1.1 Bev; and (3) the experimental cross section for $(n\pi^+\pi^-)$ production, modified from the 1.0-Bev value by an amount proportional to the change in the total inelastic cross section. The values which were used for these quantities are listed in Table II. [The notation used for cross sections is that of Sternheimer and Lindenbaum:² σ_{2T} and $\sigma_{2T,\alpha}$, when T is the isotopic spin of the initial (π,p) system and α is 1 for the $T=\frac{3}{2}$ isobar, and 2 for the $T=\frac{1}{2}$ isobar. Additional subscripts s or d refer to single or double pion production, respectively.] In this preliminary calculation the fraction of the cross section involving formation of the $T=\frac{1}{2}$ isobar, $k=\sigma_{12}/(\sigma_{11}+\sigma_{12})=\sigma_{32}/(\sigma_{31}+\sigma_{32})$, was used as a variable parameter to be determined by fitting the theoretical spectra to the experimental momentum distributions from this experiment. The best fit, as shown in Fig. 12, obtained with the values of Table II was given by $k=0.7$.

TABLE II. Cross-section values used in the preliminary isobar model calculation.

Cross section	Value	Source
$\sigma_{\pi^-,p \text{ inel}} = \frac{2}{3}\sigma_1 + \frac{1}{3}\sigma_3$	21 mb	(Brisson <i>et al.</i>) ^a
$\sigma_{\pi^+,p \text{ inel}} = \sigma_3$	17.6 mb	(Stonehill <i>et al.</i>) ^b
$R = \sigma(p\pi^-\pi^0)/\sigma(n\pi^+\pi^-)$ at 1 Bev	0.50	(Derado and Schmitz) ^c
$\sigma(n\pi^+\pi^-)$ at 1.0 Bev	10.4 mb	(Derado and Schmitz) ^c
$\sigma(n\pi^+\pi^-)$ at 1.1 Bev = 0.9(10.4)	9.5 mb	(from σ_{inel} ratio)
$k = \sigma_{12}/(\sigma_{11}+\sigma_{12}) = \sigma_{32}/(\sigma_{31}+\sigma_{32})$: retained as variable parameter		

^a See reference 28.

^b See reference 30.

^c See reference 14.

³⁰ D. Stonehill, C. Baltay, H. Courant, W. Fickinger, E. C. Fowler, H. Kraybill, J. Sandweiss, J. Stanford, and H. Taft, *Phys. Rev. Letters* **6**, 624 (1961).

TABLE III. Cross-section values used in the detailed isobar model calculation.

Cross section	Value	Source
$\sigma_{\pi^-,p}$ (total)	35.6 ± 2.0 mb	(Brisson <i>et al.</i>) ^a
$\sigma_{\pi^-,p}$ (charged elastic)	12.0 ± 1.0 mb	(Brisson <i>et al.</i>) ^a
$\sigma_{\pi^-,p}$ (neutral)	5.3 ± 0.5 mb	(Brisson <i>et al.</i>) ^b
$\sigma_{\pi^-,p}$ (neutral inelastic)	3 ± 1 mb	(Falk-Vairant and Valladas) ^a
$\sigma(\pi^+p \rightarrow p\pi^+\pi^0)$	11.0 ± 1.0 mb	(Stonehill <i>et al.</i>) ^c
$\sigma(\pi^+p \rightarrow n\pi^+\pi^+)$	2.6 ± 0.5 mb	(Stonehill <i>et al.</i>) ^c
$\sigma(\pi^+p \rightarrow$ charged mult. prod.)	4.0 ± 0.6 mb	(Stonehill <i>et al.</i>) ^c
$\sigma(\pi^-p \rightarrow p\pi^+\pi^-\pi^-)$	0.6 ± 0.3 mb	(Derado and Schmitz) ^d
$R = \sigma(p\pi^-\pi^0)/\sigma(n\pi^+\pi^-)$	0.50 ± 0.14	(Derado and Schmitz) ^d

^a See reference 28.^b See reference 31.^c See reference 30.^d See reference 14.

This result implies a strong preference (70%) for the formation of the $T = \frac{1}{2}$ isobars in order to explain the preponderance of high-momentum π^0 and low-momentum π^- observed in the ($p\pi^-\pi^0$) events of the present experiment, if the proposed $T = \frac{1}{2}$ isobaric states are assumed to occur.

Although a reasonably good qualitative fit to the momentum data was obtained by setting $k=0.7$, it is difficult to defend this choice in view of the values of the ratio which may be calculated from the measured cross sections for the individual single- and double-pion production charge states. Although these experimental cross sections are subject to appreciable error, it is nevertheless of interest to carry out a detailed isobar model calculation, with propagation of the relevant experimental errors, to determine the limits placed on the π^0 and π^- momentum spectra and on the ratio k by the best available experimental information for this energy. The input information for this more detailed isobar calculation is presented in Table III, together with the sources.

Consider first the Yale data on the π^+, p interaction³⁰; taking $\sigma^{IV} = \sigma(\pi^+p \rightarrow p\pi^+\pi^0) = (13/15)\sigma_{31} + (1/3)\sigma_{32,s} = 11.0 \pm 1.0$ mb, and $\sigma^V = \sigma(\pi^+p \rightarrow n\pi^+\pi^+) = (2/5)\sigma_{31} + (2/3)\sigma_{32,s} = 2.6 \pm 0.5$ mb, one obtains for σ_{31} the value 12.1 ± 1.3 mb and for $\sigma_{32,s}$ the value 1.5 ± 0.9 mb. Combining this latter value with $\sigma_{32,d} = 4.0 \pm 0.6$ mb, one obtains $\sigma_{32} = 5.5 \pm 1.0$ mb, the total contribution to $T = \frac{3}{2}$ scattering from the $T = \frac{1}{2}$ isobar. The ratio $k = \sigma_{32}/(\sigma_{31} + \sigma_{32})$, which is assumed to equal the ratio $\sigma_{12}/(\sigma_{11} + \sigma_{12})$ in π^-, p interactions, is then found to be 0.31 ± 0.10 . It is clear that the value 0.7 for this ratio, which gives satisfactory agreement with the measured momentum distributions, is not in good agreement with the value from cross sections measured for π^+, p interactions.

By subtracting the charged-elastic²⁸ and charge-exchange³¹ cross sections listed in Table III from the

total π^-, p cross section, one obtains a value of 21.3 ± 2.5 mb for $\sigma(\pi^-, p \text{ inelastic}) = \frac{2}{3}\sigma_1 + \frac{1}{3}\sigma_3$. With the use of $\sigma_3 = (\sigma_{31} + \sigma_{32}) = 17.6 \pm 1.7$ mb, one finds $\sigma_1 = (\sigma_{11} + \sigma_{12}) = 23.1 \pm 3.8$ mb, the total $T = \frac{1}{2}$ inelastic cross section at this energy. Assuming that the Lindenbaum-Sternheimer constant ρ , where $\rho = \sigma_{3\alpha}/2\sigma_{1\alpha}$, is the same for the $T = \frac{1}{2}$ and $T = \frac{3}{2}$ states [the same assumption as $\sigma_{12}/(\sigma_{11} + \sigma_{12}) = \sigma_{32}/(\sigma_{31} + \sigma_{32})$], one obtains for σ_{11} the value 15.9 ± 4.3 mb, and for σ_{12} the value 7.2 ± 1.9 mb. The value of the constant ρ is then 0.38 ± 0.11 .

In order to determine the fractions of σ_{12} which are associated with single- and with double-pion production, one must make use of the available information on multiple pion production in π^-, p interactions in this energy region. Unfortunately few determinations of these cross sections near 1 Bev are available, and the published values have large statistical errors. A number of assumptions must be made. It is assumed that the cross section for charged double-meson production at 1100 Mev is the same as that at 1000 Mev where a value of 3.1 ± 0.8 mb was obtained by Derado and Schmitz.¹⁴ Also it is assumed that the neutral inelastic cross section is divided between single- and double-pion production in the same ratio as the charged inelastic cross section. Using the Derado and Schmitz¹⁴ value for this ratio, one obtains a value of 3.6 ± 0.9 mb for the total double-pion production cross section in π^-, p interactions, $\sigma_{2d} = \frac{2}{3}(1 + \rho_2)\sigma_{12,d}$. By multiplying σ_{12} by the ratio $\sigma_{2d}/(\frac{2}{3}\sigma_{12} + \frac{1}{3}\sigma_{32})$ one obtains a value for $\sigma_{12,d}$. A value for $\sigma_{12,s}$ of 3.3 ± 1.5 mb is then calculated.

The remaining parameters necessary for calculation of the pion momentum distributions may be obtained from the cross section for the readily identified reaction ($\pi^-p \rightarrow p\pi^+\pi^-\pi^-$) and the ratio R of the cross sections for the charged single-pion production reactions (Table III). These are assumed to be approximately the same at 1100 Mev as at 1000 Mev. The constants in the relation for the momentum spectrum of the π^- in ($p, \pi^-\pi^0$) production,

$$d\sigma/dp = C_1 J_{\pi,1} + C_2 J_{\pi,2} + C_3 J_{\pi,3} + C_4 J_{\pi,4},$$

where the $J_{\pi,i}$ spectra are those shown in Figs. 10–11, may then be calculated from the relations published by Sternheimer and Lindenbaum.² The values obtained for the weighting factors C_i are: $C_1 = 1.13 \pm 0.38$, $C_2 = 2.06 \pm 1.12$, $C_3 = 0.30 \pm 0.24$, and $C_4 = 1.42 \pm 0.78$. The spectrum for the π^0 from the same reaction is obtained by interchanging C_1 with C_2 and C_3 with C_4 .

The relatively large values of C_2 and C_4 compared to C_1 and C_3 , even when the sizable uncertainties are considered, require a peak in the π^- momentum spectrum at higher momentum than the peak for the π^0 . This prediction of the isobar model is in disagreement with the results of this experiment.

In order to investigate the limits placed on the momentum distributions for π^- and π^0 by the initial measurement errors propagated in this detailed isobar calculation, one must consider that the error limits on the

³¹ J. C. Brisson, P. Falk-Vairant, J. P. Merlo, P. Sonderegger, R. Turlay, and G. Valladas, *Proceedings of the 1960 Annual International Conference on High-Energy Physics at Rochester* (Interscience Publishers, Inc., New York, 1960), p. 191.

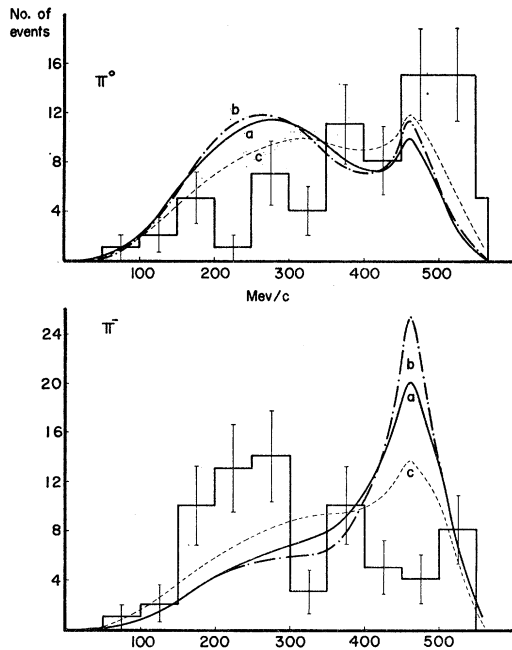


FIG. 13. Momentum distributions for the neutral and negative pions in the c.m.s. The smooth curve (a) is calculated from the extended isobar model using the best available data for all cross sections. Curves (b) and (c) indicate the highest and lowest limits on the π^- momentum peak permitted by the measurement errors in the cross-section information. The isobar model calculations assume that the low-energy $T=\frac{1}{2}$ cross section may be neglected.

C_i factors are not independent. Sets of momentum spectra were computed with the upper and lower limits for each of the following: σ (π^-, p inelastic), σ_3 , σ_{31} , σ_{32} , σ_{2a} , σ ($\pi^- p \rightarrow p\pi^+\pi^-\pi^-$), and R . The extremes in the resulting $d\sigma/dp$ distributions were then selected. The C_i factors which gave maximum and minimum momentum peaks for the π^- mesons are listed in rows (b) and (c), respectively, in Table IV, and the C_i factors obtained with the nominal values of the input parameters are listed in row (a). The momentum distributions, $d\sigma/dp = \sum C_i J_{\pi,i}$, for the π^0 and π^- are shown in Fig. 13, as calculated from the $J_{\pi,i}$ spectra of Fig. 10 in which the low-energy $T=\frac{1}{2}$ cross section contribution is neglected, and in Fig. 14 for the $J_{\pi,i}$ spectra of Fig. 11 where this contribution is included. In neither case does the isobar model provide a good fit to the experimental distributions within the limits of error determined by the available cross-section values, in spite of the apparent qualitative agreement noted above.

VII. DISCUSSION

Although the predictions of the isobar model as extended to include excitation of both $T=\frac{3}{2}$ and $T=\frac{1}{2}$ states seem to be in qualitative agreement with the kinematical features of single neutral pion production observed in this experiment, the apparent agreement does not seem to be confirmed by detailed calculations. Cross-section values available for elastic and inelastic

TABLE IV. C_i factors calculated for pion momentum distributions from the error limits on the input cross sections.

Distribution	C_1	C_2	C_3	C_4
a	1.131	2.056	0.304	1.418
b	1.293	3.145	0.007	0.105
c	0.946	0.997	1.252	1.669

π^\pm, p interactions lead to an isobar model prediction for the ratio of $T=\frac{1}{2}$ to $T=\frac{3}{2}$ isobar formation which would require a peak in the π^- momentum spectrum at a higher momentum than the peak in the π^0 spectrum. The quantitative disagreement between the model and the results of this experiment might be interpreted either as a failure of the model or as the result of biases in the experimental distributions.

The results of this experiment may be compared with results of several experiments at comparable energies. The results reported here agree well with those described by Derado and Schmitz,¹⁴ who also find predominantly fast, forward-scattered π^0 mesons, and slower π^- mesons distributed more or less isotropically in the pion-proton c.m.s. These differ somewhat from the results of Alles-Borelli *et al.*¹⁵ for a somewhat lower energy at which predominantly fast π^- mesons, largely forward-scattered, and π^0 mesons which are slower and quite isotropic in the c.m.s. have been observed. The results of Salant and his co-workers, both below¹⁶ and above¹⁷ 1 BeV, seem to agree better with the Alles-Borelli data than with the data of Derado and Schmitz and the present experiment.

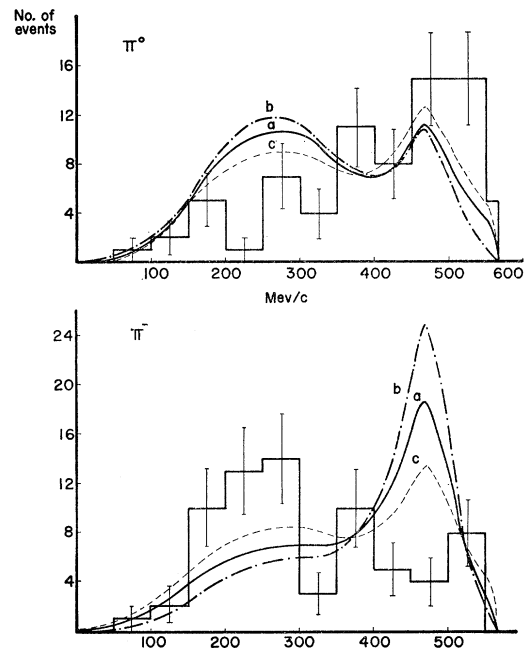


FIG. 14. Distributions showing the same information as Fig. 13, except that the isobar model calculation includes the low-energy $T=\frac{1}{2}$ cross-section contribution.

The question immediately arises as to whether the somewhat stringent identification procedure for the neutral pions used in the present experiment might introduce a selection bias favoring identification of fast neutral pions and/or slow negative pions in the reaction.

The possibility that scanning for conversion electron pairs which follow π^0 decay might introduce such a selection bias should not be great, inasmuch as each π^0 decay produces two photons moving in opposite directions in the decay c.m.s., so that in the laboratory system the energy partition between the two photons will be quite asymmetric. The effect of this energy asymmetry should be more than enough to smear out the energy difference between decay photons from π^0 mesons whose momenta differ by only ~ 250 Mev/c. Furthermore, 25 of the 70 events used in this sample were selected independently by identifying Dalitz-decay electron pairs, for which the scanning bias would be absent, and the momentum distributions for these events agree well with the entire sample (Fig. 7).

The large number of high-energy π^0 's observed in this experiment could also be explained by assuming that an appreciable contamination of double-pion production events is present in the sample. Since the available energy in double-pion production is distributed among a larger number of particles, the average π^- momentum in these events should be lower than in single-pion production events and in general the computed neutral particle momentum should be higher. Double production events of the types $(p\pi^-\pi^0\pi^0)$ and $(n\pi^+\pi^-\pi^0)$ may have associated electron pairs and can be eliminated only by kinematic analysis. Definite identification of such double production events is difficult since two neutral particles are present. One may, however, compare the single to double production ratio $\sigma(p\pi^-\pi^0)/[\sigma(p\pi^-\pi^0\pi^0)+\sigma(n\pi^+\pi^-\pi^0)]$, observed in this experiment with the ratio found in other experiments. This ratio is 3.75 for type-A events; if the independently selected type-B events are included, the ratio becomes 3.68 (see Table I). In the experiment of Alles-Borelli *et al.* the ratio was $190/(8+43)=3.72$. The excellent agreement here may be somewhat fortuitous; the value obtained by Derado and Schmitz is 2.1. If the latter ratio were taken to be correct, then the number of $(p\pi^-\pi^0)$ events expected in the present experiment would be $0.68(89)=60$, compared to the 70 events now included. The indicated contamination of double production events in this experiment is 14%, probably not sufficient to explain the differences in this experiment and the isobar model. The number of high-momentum π^- cannot be increased by removing a contamination of this type. However, it should be noted that in each of the experiments discussed, and particularly in the present experiment, the statistical uncertainties are appreciable, and the possibility of such contamination cannot be ruled out.

One must turn then to the possibility that there is a

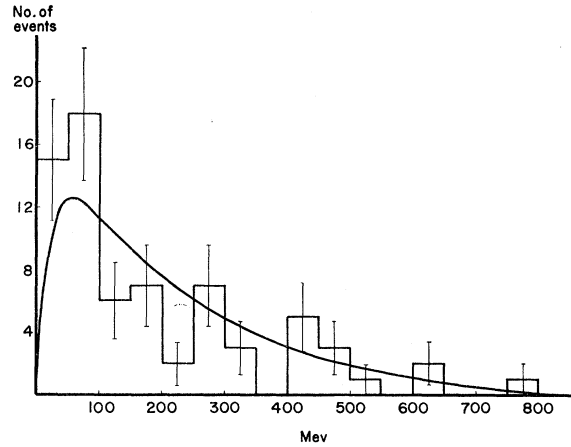


FIG. 15. Laboratory momentum distribution of the proton from the $(p\pi^-\pi^0)$ production reaction. The smooth curve is plotted from an equation of Chew and Low assuming constant $\pi\pi$ cross section.

real difference between the results of the different experiments carried out in the range 960–1100 Mev. One conceivable explanation would be that the mechanism responsible for single-pion production is quite energy sensitive in this range; some support for this point of view may be found in the findings of Salant and his colleagues¹⁷ that the neutron angular distribution from the $(n\pi^+\pi^-)$ reaction shifts from near isotropy in the c.m.s. at 960 Mev to a predominant backward scattering at 1100 Mev. An alternative explanation might be that the differences lie in the selection procedures used to identify the single production charge states in the different experiments. As noted above, both Derado and Schmitz and the present experiment were designed to minimize the problems of event identification in the momentum region of kinematic ambiguity, where track density separation of the positive particles is also difficult. The ratio of $(n\pi^+\pi^-)/(p\pi^-\pi^0)$ single production events found by Derado and Schmitz was 2.0 ± 0.5 ; the same ratio measured by Alles-Borelli *et al.* was 1.25 ± 0.16 , which is only consistent with the first at the 15% confidence level. There is evidence²² that the number of kinematically ambiguous identifications can be quite appreciable, and it may perhaps be possible that some events could have been identified as $(n\pi^+\pi^-)$ in one experiment and as $(p\pi^-\pi^0)$ in another; this could affect the neutral particle distributions appreciably.

In any case, each of the experiments in this energy range presents features which are not predicted by the isobar model. For example, the differences between the nucleon laboratory kinetic energy spectra observed for single-pion production and the isobar model predictions have been discussed in some detail,⁶⁻⁷ and the conclusion has been drawn that this feature of the data may be explained by assuming that a strong pion-pion interaction initiates the reaction process. A number of features of pion-nucleon interactions near 1 Bev are indicative of the importance of interactions at large

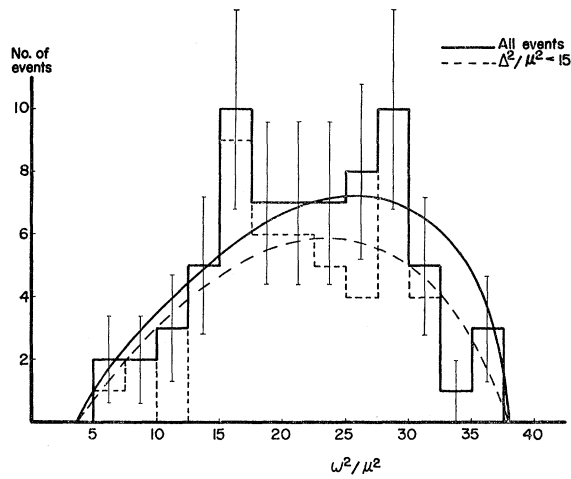


FIG. 16. Distributions of ω^2 , the square of the total energy of the $(\pi^-\pi^0)$ in their barycentric system, in units of μ^2 , the square of the pion rest mass energy. Curves are plotted from Chew-Low theory for constant $\sigma_{\pi\pi}$. The solid curves and histograms include all events, while the dashed curves are restricted to events in which the square of the momentum transfer was $<15 \mu^2$.

impact parameters. Among the relevant features in single-pion production at 1100 Mev is the backward peaking of the nucleon angular distribution. The effects can be explained most easily by assuming an interaction between the incoming pion and the pion cloud of the nucleon. One striking result of such an interaction is a low-energy peak in the laboratory kinetic-energy spectrum of the nucleons, first predicted by Goebel.³² The laboratory kinetic-energy spectrum for the protons from the present experiment is peaked at considerably lower than the ~ 185 -Mev value predicted by the isobar model and, as shown in Fig. 15, agrees reasonably well with the distribution computed by integrating the Chew-Low equation,³³

$$\frac{\partial^2 \sigma}{\partial \Delta^2 \partial \omega^2} \xrightarrow{\Delta^2 \rightarrow -\mu^2} \frac{f^2}{2\pi} \frac{\Delta^2/\mu^2}{(\Delta^2 + \mu^2)^2} \frac{\omega(\frac{1}{4}\omega^2 - \mu^2)^2}{q_{in}^2} \sigma_{\pi\pi}(\omega),$$

over the energy variable ω under the assumption that the pion-pion cross section is independent of ω in this region. Here Δ is the four-momentum transfer from the target pion to the nucleon, μ is the pion rest mass, ω the total energy of the two-pion state in the pion-pion c.m.s., f^2 the renormalized pion-nucleon coupling constant, q_{in} the momentum of the incident pion in the laboratory frame of reference, and $\sigma_{\pi\pi}(\omega)$ the $\pi\pi$ cross section.

Evidently the same equation may be used to calculate the ω^2 spectrum by integrating over values of Δ^2 . The pion-pion total energy ω is the sum ($Q_{\pi\pi} + 2\mu$); the experimental spectrum of ω^2 in units of μ^2 , the square of the pion rest mass, is shown in Fig. 16 together with

the Chew-Low curve calculated for constant $\sigma_{\pi\pi}$. The agreement is if anything, somewhat better than in the experiment of Rushbrooke and Radojicic,¹⁸ and reflects the fact that momentum transfer is low and hence consistent with a "peripheral" collision in the great majority of cases.

The apparent peaking of the ω^2 distribution above the constant pion-pion cross section curve in the intervals $15 \mu^2 < \omega^2 < 17.5 \mu^2$ and $27.5 \mu^2 < \omega^2 < 30 \mu^2$ is of particular interest. This peaking seems most pronounced for the events which correspond to low-momentum transfers with $\Delta^2 < 15 \mu^2$, as would be expected for an effect associated primarily with peripheral collisions. It is known^{18,30} that the $T=1$ " ρ " dipion state with $\omega^2 = 29 \mu^2$ is excited in single-pion production, and there has been a recent report from Saclay³⁴ of a $T=1$ " ζ " dipion state with $\omega^2 = 17 \mu^2$ observed for the $\pi^+\pi^0$ system. Although the limited statistics of the present experiment call for considerable caution in the interpretation of pion-pion effects, the evidence presented here at least suggests strongly that both reported dipion resonances are excited with comparable probability in the $\pi^-\pi^0$ system at the energy of this experiment.

A comparison of the ω^2 distribution with the statistical model prediction, Fig. 17, illustrates the rather poor agreement between experiment and theory. The spectrum predicted by the isobar model is expected to be similar to that for the statistical model. This disagreement also appears in the c.m.s. momentum distribution of the proton, Fig. 6. The presence of evidence for the pion-pion interaction and of the (π, N) Q -value peaks associated with the $T=J=\frac{3}{2}$ isobaric state observed at this energy does not indicate a contradiction. As

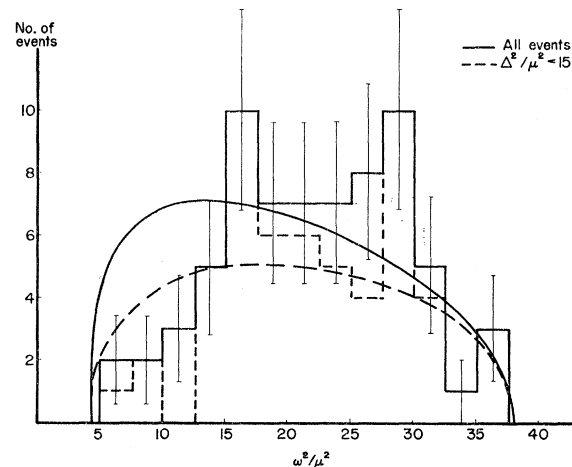


FIG. 17. Distribution of ω^2 , the square of the total energy of the $(\pi^-\pi^0)$ in their barycentric system, with the statistical model predictions plotted for comparison. Solid curves and histograms include all events, while the dashed curves are restricted to events in which the square of the momentum transfer was $<15 \mu^2$.

³² C. Goebel, Phys. Rev. Letters **1**, 337 (1958).

³³ G. F. Chew and F. E. Low, Phys. Rev. **113**, 1640 (1959).

³⁴ R. Barloutaud, J. Heughebaert, A. Levique, J. Meyer, and R. Omnes, Phys. Rev. Letters **8**, 32 (1962).

Selleri⁸ has pointed out, the c.m. energy of the secondary pions from the $\pi-\pi$ interaction would be such that in many cases a rescattering in the $(\frac{3}{2}, \frac{3}{2})$ state of one of these pions from the nucleon might occur. This might lead to the observed (π, N) Q -value peaks and the corresponding peaks in pion momentum spectra.

The principal kinematic features (momenta and Q values) observed in this and in other experiments¹⁶ at this energy are not necessarily indicative of the excitation of the $T=\frac{1}{2}$ resonance pion-nucleon states, since the momentum spectra of the recoil pion from $T=\frac{1}{2}$ isobar production and the decay pion from $T=\frac{3}{2}$ isobar production are expected to be similar. It thus appears unnecessary on the basis of the present evidence to invoke the postulated $T=\frac{1}{2}$ isobaric states to explain the observed effects, although excitation of these states is not ruled out. In view of increasing interest in theories involving π^* , K^* , and Y^* resonant systems³⁵ the experimental evidence for assuming more than one N^* state should be carefully examined.

It would seem that the kinematics of single neutral pion production in a limited sample, selected so as to avoid misidentification of the neutral particle, are in rather serious disagreement with the detailed predictions of charge states obtained from a simple isobar model which assumes the importance of $T=\frac{1}{2}$ nucleon isobars. On the other hand, the recoil nucleon energies

³⁵ H. P. Dürr and W. Heisenberg, *Z. Naturforsch.* **16A**, 726 (1961).

and the pion-pion energy distribution are consistent with the assumption that a strong pion-pion interaction initiates the reaction. The features of the angle and momentum distributions which suggest a strong pion-nucleon interaction might be qualitatively explained in terms of rescattering of the pions by the recoil nucleon in the $T=\frac{3}{2}$ pion-nucleon state. In view of the limited statistics of the experiment, no attempt has been made to calculate the pion-pion interaction cross section.

The selection technique for $(p\pi-\pi^0)$ events which was used in this experiment appears to be a useful method for checking the results of pion-production studies in which other selection criteria are used. The number of events obtained with this method might be increased considerably if a larger bubble chamber could be used.

ACKNOWLEDGMENTS

We wish to thank the Alvarez Bubble Chamber Group of the University of California Lawrence Radiation Laboratory for their kindness in making the data of this experiment available. Dr. H. Bradner and Robert West provided invaluable assistance.

It is a pleasure to express our indebtedness to Professor J. G. Dardis for his contribution to the early phases of this work, and to Gunter Brunhart for many helpful suggestions. The assistance of Claudine Gall in scanning and analysis was invaluable. The cooperation of the University of Kentucky computing center is acknowledged with appreciation.

Multiple Meson Production in Proton-Proton Collisions at 2.85 BeV*

E. L. HART, R. I. LOUITT, D. LUERS,† T. W. MORRIS, W. J. WILLIS, AND S. S. YAMAMOTO

Brookhaven National Laboratory, Upton, New York

(Received December 1, 1961)

Measurements have been made on 753 four-prong events obtained by exposing the Brookhaven National Laboratory 20-in. liquid hydrogen bubble chamber to 2.85-BeV protons. The partial cross sections observed for multiple meson production reactions are: $pp+- (p+p \rightarrow p+p+\pi^++\pi^-)$, 2.67 ± 0.13 ; $pn+ +-$, 1.15 ± 0.09 ; $pp+-0$, 0.74 ± 0.07 ; $d+ +-$, 0.06 ± 0.02 ; four or more meson production, 0.04 ± 0.02 , all in mb. Production of two mesons appears to occur mainly in peripheral collisions with relatively little momentum transfer. In cases of three-meson production, however, the protons are typically deflected at large angles and are more strongly degraded in energy. The $\frac{3}{2}$, $\frac{3}{2}$ pion-nucleon resonance dominates the interaction; there is some indication that one or both of the $T=\frac{1}{2}$, pion-nucleon resonances also play a part. The recently discovered resonance in a $T=0$, three-pion state appears to be present in the $pp+-0$ reaction. Results are compared with the predictions of the isobaric nucleon model of Sternheimer and Lindenbaum, and with the statistical model of Cerulus and Hagedorn. The cross section for the reaction $\pi^0+p \rightarrow \pi^++\pi^-+p$ is derived using an expression from the one-pion exchange model of Drell.

I. INTRODUCTION

THE scattering of nucleons by nucleons at high energies has been studied extensively in recent years. Such features of the interaction as the total and elastic cross sections have been investigated by experi-

mental groups using electronic counters.¹ However, this technique is of limited utility in its application to inter-

* Work performed under contract with the U. S. Atomic Energy Commission.

† Max Planck Institute, Munich, West Germany.

¹ F. F. Chen, C. P. Leavitt, and A. M. Shapiro, *Phys. Rev.* **103**, 211 (1956); B. Cork, W. A. Wenzel, and C. W. Causey, *Phys. Rev.* **107**, 859 (1957); M. J. Longo, J. A. Helland, W. N. Hess, B. J. Moyer, and V. Perez-Mendez, *Phys. Rev. Letters* **3**, 568 (1959); M. J. Longo, thesis, University of California Radiation Laboratory Report UCRL-9497, 1961 (unpublished); G. Von Dardel, D. H. Frisch, R. Mermod, R. H. Milburn, P. A. Piroué, M. Vivargent, G. Weber, and K. Winter, *Phys. Rev. Letters* **5**, 333 (1960).